ISSN 1674-1056
http://cpb.iphy.ac.cn
http://iopscience.iop.org/cpb
中国物理 B
Chinese Physics
中国物理
Chinese Physics B

Ground-state phase diagram of the dimerizedspin-1/2 two-leg ladder

Cong Fu(傅聪), Hui Zhao(赵晖), Yu-Guang Chen(陈宇光), and Yong-Hong Yan(鄢永红)
Citation: Chin. Phys. B, 2021, 30 (**8**): 087501. DOI: 10.1088/1674-1056/abec31
Journal homepage: http://cpb.iphy.ac.cn; http://iopscience.iop.org/cpb

What follows is a list of articles you may be interested in

Emergent O(4) symmetry at the phase transition from plaquette-singlet to antiferromagnetic order in quasi-two-dimensional quantum magnets

Guangyu Sun(孙光宇), Nvsen Ma(马女森), Bowen Zhao(赵博文), Anders W. Sandvik, and Zi Yang Meng(孟子杨)
Chin. Phys. B, 2021, 30 (**6**): 067505. DOI: 10.1088/1674-1056/abf3b8

Absence of magnetic order in dichloro [1,2-bis (diphenylphosphino) ethane] nickel^{2+} single crystal

Shuaiqi Ma(马帅奇), Linlin An(安琳琳), and Xiangde Zhu(朱相德)
Chin. Phys. B, 2021, 30 (**5**): 057501. DOI: 10.1088/1674-1056/abe233

Magnetocaloric effect and critical behavior of the Mn-rich itinerant material Mn_3GaC with enhanced ferromagnetic interaction

Pengfei Liu(刘鹏飞), Jie Peng(彭杰), Mianqi Xue(薛面起), Bosen Wang(王铂森)
Chin. Phys. B, 2020, 29 (**4**): 047503. DOI: 10.1088/1674-1056/ab7da1

Interplay between spin frustration and magnetism in the exactly solved two-leg mixed spin ladder

Yan Qi(齐岩), Song-Wei Lv(吕松玮), An Du(杜安), Nai-sen Yu(于乃森)
Chin. Phys. B, 2016, 25 (**11**): 117501. DOI: 10.1088/1674-1056/25/11/117501

Exact solution of Heisenberg model with site-dependent exchange couplings and Dzyloshinsky-Moriya interaction

Yang Li-Jun, Cao Jun-Peng, Yang Wen-Li
Chin. Phys. B, 2015, 24 (**10**): 107502. DOI: 10.1088/1674-1056/24/10/107502

Ground-state phase diagram of the dimerized spin-1/2 two-leg ladder*

Cong Fu(傅聪)[1], Hui Zhao(赵晖)[1,†], Yu-Guang Chen(陈宇光)[1], and Yong-Hong Yan(鄢永红)[2]

[1] School of Physics Science and Engineering, Tongji University, Shanghai 200092, China
[2] School of Mathematical Information, Shaoxing University, Shaoxing 312000, China

(Received 31 December 2020; revised manuscript received 31 December 2020; accepted manuscript online 5 March 2021)

Dimerized spin-1/2 ladders exhibit a variety of phase structures, which depend on the intra-chain and inter-chain spin exchange energies as well as on the dimerization pattern of the ladder. Using the density matrix renormalization group (DMRG) algorithm, we study critical properties of the bond-alternating two-leg Heisenberg spin ladder with diagonal interaction $J_\times$. Two types of spin systems, staggered dimerized antiferromagnetic ladder and columnar dimerized ferro-antiferromagnetic couplings ladder, are investigated. To clarify the phase transition behaviors, we simultaneously analyze the string order parameter (SOP), the twisted order parameter (TOP), as well as a measurement of the quantum information analysis. Based on measuring this different observables, we establish the phase diagram accurately and give the fitting functions of the phase boundaries. In addition, the phase transition of cross-coupled spin ladder (in the absence of intrinsic dimerization) is also discussed.

Keywords: spin ladder, density matrix renormalization group, Heisenberg model, quantum phase transition

PACS: 75.10.Jm, 75.10.Pq, 75.40.Mg, 75.50.Ee **DOI:** 10.1088/1674-1056/abec31

1. Introduction

Low dimensional spin systems have become one of the main research topics in condensed matter physics in the last few decades. This kind of system is dominated by strongly correlated effects and exhibits intensive quantum fluctuations in the ground state. In particular, quantum spin ladder provides an important theoretical tool to study the crossover between one-dimensional chains and two-dimensional planes. Spin ladders are known to exhibit interesting quantum critical behavior. For example, the two-leg spin ladder $SrCu_2O_3$ shows a gap between the lowest singlet and the triplet states while the three-leg spin ladder $Sr_2Cu_3O_5$ is gapless.[1] The quantum phase transition (QPT) of spin ladders has attracted numerous interest. With improvement of experimental techniques, some spin ladder compounds can be realized close to the quantum critical region, such as $CuBr_4$[2] and Ba_2CuTeO_6,[3–6] which makes efforts to understand QPTs in depth.

For a spin ladder considering the nearest intrachain coupling J and interchain rung coupling $J_\perp$, it has been a common view that the phase diagram consists of two quantum phases: the rung-singlet (RS) phase and the Haldane phase, and the critical points is at $J_\perp = 0$. When the interchain diagonal coupling $J_\times$ is introduced, the QPTs could be complicated. By renormalization group, Starykh and Balents[7] proposed that the transition between the RS phase and the Haldane phase cannot occur at weak couplings and predicted two immediate dimer phases, named the columnar dimer(CD) phase and the staggered dimer (SD) phase, in the phase diagram. When the rung coupling $J_\perp$ is strong enough, the dimerization would disappear and these two dimer phases are degenerate. When $J_\perp$ is not so strong, the rung singlet brings less free energy, therefore the CD phase is more stable for the thermodynamic limit.[8] However, the existence of these dimer phases has been disputed,[9–12] while other works[13,14] have provided evidence that confirms the presence of the dimer phases.

On the other hand, the spin-Peierls transition has been obtained in some spin ladder compounds.[15] The ground state of these materials can be described by a dimerized resonating valence bond (RVB) state:[16] ladders with odd legs correspond to long-range RVB states, while ladders with even legs correspond to short-range RVB states. Since there exists varieties of dimerized topological configurations in spin ladder, it exhibits rich scenarios of quantum ordered phases and quantum critical phenomena. The dimerized spin ladder has been studied numerically earlier.[17–21] In this work, we study the $S = 1/2$ two-leg dimerized spin ladder considered with the diagonal coupling $J_\times$ by the powerful density matrix renormalization group (DMRG)[22,23] method. We introduce intrinsic dimerization to stabilize the fragile dimer phases and try to understand the influence of diagonal coupling $J_\times$ on the quantum phase transition in the dimerized spin ladder. In particular, when the dimerization is set to be zero, the model is reduced to the cross-coupled ladder, which could enable us to find any clues of existence of dimer phases in a cross-coupled ladder.

The paper is organized as follows. Firstly we introduce the Hamiltonian of the dimerized spin ladder and our finite-

*Project supported by the National Natural Science Foundation of China (Grant Nos. 11474218 and 11575116).
†Corresponding author. E-mail: zhaoh@fudan.edu.cn
© 2021 Chinese Physical Society and IOP Publishing Ltd

size DMRG algorithm. Secondly we compute SOP, TOP and entanglement entropy to obtain a precise estimate of the phase boundary. Then we demonstrate the ground-state diagrams based on our numerical results. Finally, we discuss the cross-coupled spin ladder situation and demonstrate the ground-state diagrams as well. A summary is given in the last section.

2. Model and methods

The Hamiltonian of the bond-alternating two-leg spin ladder with diagonal frustrations is given by

$$H = \sum_{\alpha=1,2}\sum_{l} J_\alpha(l)\boldsymbol{S}_{\alpha,l}\cdot\boldsymbol{S}_{\alpha,l+1} + J_\perp\sum_{l}\boldsymbol{S}_{1,l}\cdot\boldsymbol{S}_{2,l} + J_\times\sum_{l}(\boldsymbol{S}_{1,l}\cdot\boldsymbol{S}_{2,l+1}+\boldsymbol{S}_{1,l+1}\cdot\boldsymbol{S}_{2,l}), \quad (1)$$

where $\boldsymbol{S}_{\alpha,l}$ denotes a spin-1/2 operator at site l of the α-th leg. $J(>0)$ and $J_\perp$ are the exchange interactions on legs and rungs, respectively; $J_\times$ is the diagonal exchange coupling between the legs. For convenience, hereafter we set $J = 1.0$. Finally, the dimerization patterns are defined as

$$J_\alpha(l) = J[1+(-1)^{l+\alpha}\delta] \quad \text{(staggered)}, \quad (2)$$

$$J_\alpha(l) = J[1+(-1)^{l}\delta] \quad \text{(columnar)}. \quad (3)$$

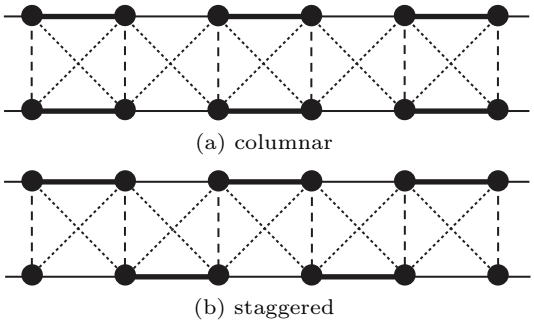


Fig. 1. Pictorial representation of the dimerized two-leg spin ladder chain. Solid dots represent spin $S = 1/2$ sites. The bond alternation with strong coupling $J(1+\delta)$ and weak coupling $J(1-\delta)$ in the leg direction are marked with bold and thin lines, respectively. In the rung direction, dashed and dotted lines represent the rung coupling $J_\perp$ and diagonal coupling $J_\times$, respectively. Dimerization patterns: (a) columnar, (b) staggered.

Our objective in this paper is to obtain the ground state phase diagram of the dimerized two-leg spin ladder in the presence of diagonal frustrations. We perform the finite-size DMRG[22,23] algorithm to study the ground state properties, and periodic boundary conditions (PBC) are applied to reduce the boundary effect. In contrast to the previous DMRG calculations which compute the vanishing of the gap directly, we mainly calculate the string order parameter (SOP),[12,13] the twist order parameter (TOP)[24,25] and block-block entanglement entropy to calculate the phase boundary separating different insulating states, and determine accurately the phase diagram. We take L to denote the ladder length so the number of sites is $N = 2L$, and rungs up to $L = 128$ were used in our studies. The convergence tests as functions of number of states kept and system size were carefully performed. The largest number of states kept in the calculation was $m = 1600$ per block, the weight of the discarded states was typically about 10^{-5}–10^{-8} depending on the parameters whether the system is in its critical state.

3. Antiferromagnetic interchain interaction

For dimerized spin ladders with two legs, the models that may have critical phases for certain configurations of the microscopic parameters are the staggered antiferromagnetic ladder and the columnar ferromagnetic ladder. We begin by presenting the results for the spin-1/2 antiferromagnetic two-leg ladders with staggered dimerization. With the increasing rung coupling, the system undergoes a phase transition from the SD phase to the RS phase, and the critical line satisfies the behavior of $J_\perp \sim \delta^{2/3}$ approximately when $J_\times = 0$.[26] The SD and RS phases can be identified by two distinct string order parameters (SOPs) O_{odd} and O_{even}. The SOP was first introduced by den Nijs and Rommelse[27] to distinguish the different gapped phases in the $S = 1$ Heisenberg chain, in which there is no local symmetry breaking, and therefore cannot be distinguished by the conventional Landau order parameter. For a two-leg ladder, the form of SOP is generalized as[28]

$$O^z_{\text{odd/even}} = -\lim_{|n-m|\to\infty}\langle S^z_{\text{rung/diag}}(n) \times \exp\left[\mathrm{i}\pi\sum_{l=n+1}^{m-1} S^z_{\text{rung/diag}}(l)\right] S^z_{\text{rung/diag}}(m)\rangle, \quad (4)$$

where $S^z_{\text{rung}}(l) = S^z_1(l)+S^z_2(l)$ and $S^z_{\text{diag}}(l) = S^z_1(l)+S^z_2(l+1)$.

It is known that for a determined state, one of the $O^z_{\text{odd/even}}$ has a finite value while the other vanishes. This is related to the topological parity of the valence-bond-solid (VBS) state. If n_{VBS} (the number of the valence bonds cut by vertical line) is odd, $O^z_{\text{odd}} \neq 0$; otherwise $O^z_{\text{even}} \neq 0$. Therefore, the intersection of the curves of two distinct string order parameters implies the critical point in the case of finite ladders. In order to reduce the boundary effects, we fix site $n = L/4$ in Eq. (4) and let site $m = 3L/4$ exist in our calculations. Our numerical results of $O^z_{\text{odd/even}}$ for various system lengths L as functions of $J_\perp$ have been demonstrated in Fig. 2. For better illustration, we set $\delta = 0.5$ and several values of $J_\times$ have been taken into account. In Fig. 2, one can distinguish a phase transition to separate two different phases distinctly. As the ladder is instinctively staggered-dimerized, the ground state for small $J_\perp$ should be SD state, there exist $O^z_{\text{odd}} \neq 0$ and $O^z_{\text{even}} = 0$. When $J_\perp$ gets larger and goes beyond the phase transition point, one has $O^z_{\text{odd}} = 0$ and $O^z_{\text{even}} \neq 0$, which implies the RS state. Comparing the results of different $J_\times$, it is explicit that the critical points $J_\perp$ of the SD–RS phase transition are larger for larger

$J_\times$. These indicate that the antiferromagnetic diagonal frustration favors the SD state, resulting in a large $J_\perp$ to drive the system from SD state into RS state. Furthermore, one can find that the curves of different sizes almost coincide at far away from the phase transition point. In the vicinity of the phase boundary, the $O^z_{\rm odd}(O^z_{\rm even})$ curves vary even more steeply as the system size increases. In addition, there exists a crossover point among these $O^z_{\rm odd}(O^z_{\rm even})$ curves of different L, and this crossover point can be considered as an estimate of the position of phase boundary because the curves expect to be perpendicular at the thermodynamic limit. Corresponding to our numerical results, the phase boundaries exist roughly at $J_\perp \approx 1.231, 1.279, 1.369$ for $J_\times = 0, 0.2, 0.5$, respectively.

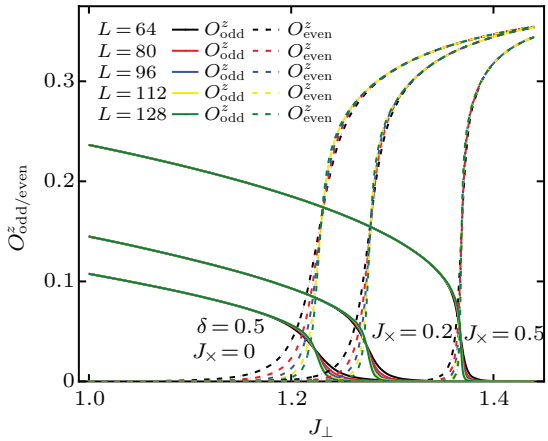


Fig. 2. Evolution of string order parameters $O^z_{\rm odd/even}$ for different system sizes L and diagonal couplings $J_\times$. The dimerization strength parameter is set to $\delta = 0.5$.

Although SOP can distinguish the phase transition between the different states, it is difficult to determine the precise location of the critical points because the crossover point is difficult to converge. For this purpose we consider another non-local twist order parameter (TOP),[24,25] which can distinguish different VBS states in one-dimensional spin systems more directly and precisely. For a two-leg ladder, the TOPs are defined as follows:

$$z_{\rm rung}(L) = \left\langle \exp\left[{\rm i}\frac{2\pi}{L}\sum_{n=1}^{L} n(S^z_{1,n}+S^z_{2,n})\right]\right\rangle, \tag{5}$$

$$z_{\rm diag}(L) = \left\langle \exp\left[{\rm i}\frac{2\pi}{L}\sum_{n=1}^{L} n(S^z_{1,n+1}+S^z_{2,n})\right]\right\rangle. \tag{6}$$

The operator $z_{\rm rung}$ $(z_{\rm diag})$ is defined for ladders under periodic boundary conditions, which converges to -1 $(+1)$ in the SD phase and to $+1$ (-1) in the RS phase. It has turned out that the TOP operators perform well in the task of accurately locating the phase boundaries of dimerized chains.[24]

In the $L\to\infty$ limit, the saturation values of $(z_{\rm rung}, z_{\rm diag})$ are expected as $(-1,1)$ and $(1,-1)$ for the SD and RS regions, respectively. In Fig. 3, we show the numerical results for $\delta = 0.5$ and $J_\times = 0.0, 0.2, 0.5$. In order to reduce the clutter caused by too many curves, only $z_{\rm diag}$ for $J_\times = 0.5$ is presented in Fig. 3 since the values of $z_{\rm rung}$ are approximately equal to $-z_{\rm diag}$. For small rung coupling $J_\perp$, $z_{\rm rung}$ tends toward -1 as the system size increases, and $z_{\rm diag}$ tends toward 1, consistent with the SD state ($n_{\rm VBS}$ is odd). For large $J_\perp$, $z_{\rm rung}$ converges to 1 and $z_{\rm diag}$ converges to -1, which indicates the existence of the RS state ($n_{\rm VBS}$ is even). It has been revealed that $z_{\rm rung/diag}$ changes signs when the parity of $n_{\rm VBS}$ changes. Therefore, the location of the transition point between SD and RS phase can be estimated by the crossing point of $z_{\rm rung}$ and $z_{\rm diag}$, where $z_{\rm rung} = z_{\rm diag} = 0$. In the inset of Fig. 3, we show the size dependence of the SD-RS boundaries determined by the conditions $z_{\rm rung}(z_{\rm diag}) = 0$. From finite-size scaling, we find the critical coupling $J_\perp \approx 1.223$, 1.274, 1.367 for $J_\times = 0.0$, 0.2, 0.5, respectively. One should note that these curves of $z_{\rm rung/diag}$ with different system sizes also intersect at one point, which is consistent with the extrapolation results.

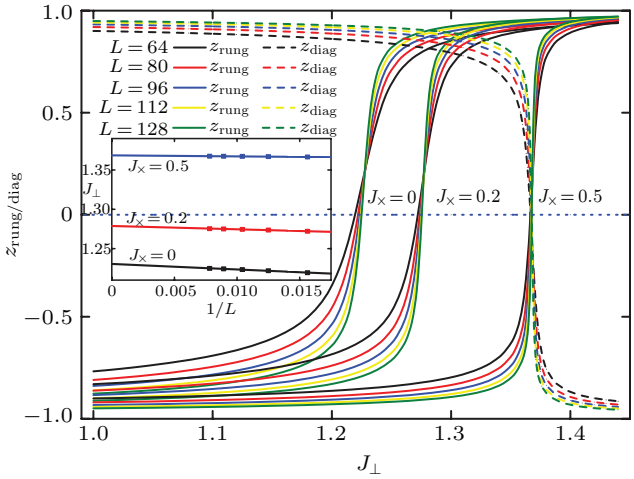


Fig. 3. Behavior of twist order parameter $z_{\rm rung/diag}$ across the phase boundary for different system sizes L and diagonal couplings $J_\times$. The dimerization strength parameter is set to $\delta = 0.5$. The inset shows a linear extrapolation of the critical values with the inverse of system size $1/L$.

In recent years, various types of quantum entropies[29–34] have been proven with an effective and accurate method for determining phase boundaries. In the beginning stage, the concept of entanglement is introduced to depict nonlocal correlations in a quantum system. If a system is divided into two separate subsystems A and B, then the reduced density matrix $\widehat{\rho}_A$ of subsystem A can be constructed by integrating out the degrees of freedom of subsystem B. Then, the quantum entanglement is described by the von Neumann entropy

$$S_A = -{\rm Tr}\widehat{\rho}_A \log_2 \widehat{\rho}_A = -\sum_\alpha \rho_\alpha \log_2(\rho_\alpha), \tag{7}$$

where ρ_α are the eigenvalues of the reduced density matrix $\widehat{\rho}_A$. Here, we apply the quantum information analysis of the phase diagram by calculating the so-called block-block entanglement (the system is divided into two equal subsystems). In Fig. 4, we present the block-block entanglement $S_{\rm BB}$ as functions of $J_\perp$. We can find that $S_{\rm BB}$ firstly increases and then

decreases as $J_\perp$ increases, developing a peak at a critical point as the nature of the ground state changes, and the location of maximum corresponds to the phase boundary separating SD and RS phases. From finite-size scaling, we obtain the critical coupling $J_\perp \approx 1.225, 1.275, 1.367$ for $J_\times = 0.0$, 0.2, 0.5, respectively. These results are in good agreement with the $z_{\text{rung/diag}}$ results described above.

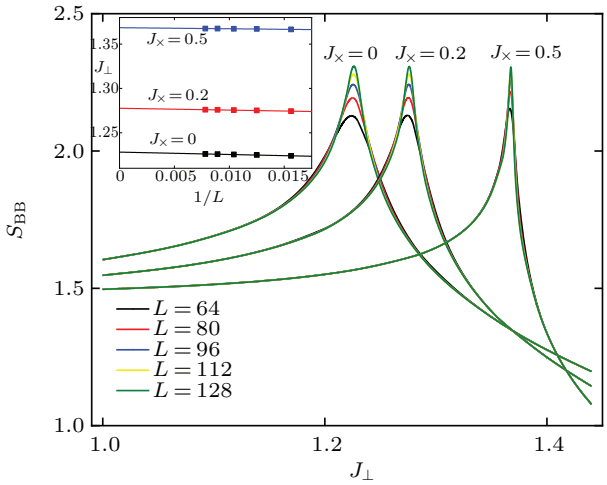


Fig. 4. Block-block entropy entanglement S_{BB} as a function of $J_\perp$ for different system sizes L and diagonal couplings $J_\times$. The dimerization strength parameter is set to $\delta = 0.5$. The inset shows a linear extrapolation of the critical values with the inverse of system size $1/L$.

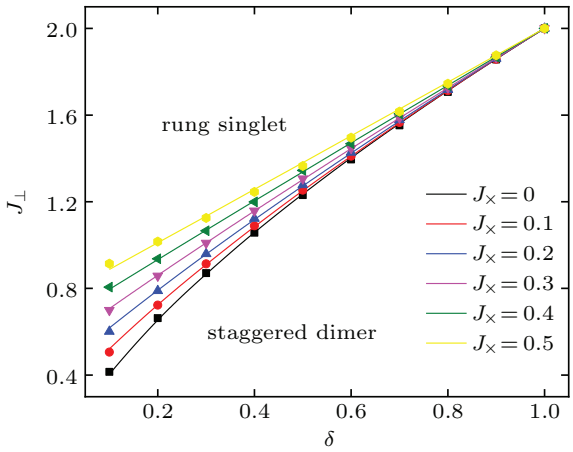


Fig. 5. Ground-state phase diagram of antiferromagnetic spin ladder with staggered dimerization. The simulation results are denoted by symbols and the fitting curves by the solid lines, respectively.

Varying the interaction energies, we determine the full ground-state phase diagram of the staggered dimerized antiferromagnetic spin ladder in the thermodynamic limit. Figure 5 shows the ground state phase diagram obtained from our TOP calculations in the δ–$J_\perp$ plane, where δ is varied from 0.1 to 1. The symbols are the numerical results and solid lines are the fitting function written as

$$J_\perp = 2.0[\delta - 0.776(1.0-\delta)\cdot J_\times]^{0.695+0.640\cdot J_\times}. \quad (8)$$

If we ignore the terms consisting of $J_\times$, the fitting function can be regarded as $J_\perp \sim \delta^{0.695}$, which is in good agreement with the earlier $J_\perp \sim \delta^{2/3}$ results. In Fig. 5, the SD plane expands as $J_\times$ is larger, which indicates that the ladder is more likely to be at the SD state when $J_\times$ is introduced and demands a larger $J_\perp$ to transfer to RS state. The curves converge at $J_\perp = 2$ when $\delta = 1$ as the spin ladder changes to the so-called "snake model" which can be solved exactly.

4. Ferromagnetic interchain interaction

On the other hand, many efforts have been devoted to studying the effects of competing interactions on low-dimensional systems, such as the competition of on-site Coulomb repulsion versus nearest-neighbor repulsion in electronic systems, the competition between ferromagnetic and antiferromagnetic interactions in spin systems, and so on. Such investigations can be interesting both for discovering possibility new phases theoretically and explaining the corresponding experimental phenomena. From this point of view, we consider a two-leg quantum spin ladder with antiferromagnetic interactions along the legs and ferromagnetic couplings along the rungs. Furthermore, the intra-chain antiferromagnetic couplings are bond alternating in a columnar configuration because the CD phase is generally more stable than SD phase, and this order parameter is available when the inter-chain couplings are ferromagnetic. Meanwhile, there exists a phase transition from CD phase to Haldane phase when the magnitude of rung coupling $J_\perp$ exceeds a certain critical value. We determine this critical lines in the quantum phase diagram using the same numerical methods and procedures discussed above, as shown in Fig. 6. In this case, the initial dimer pattern is set to be columnar, the inter-chain couplings $J_\perp < 0$ and $J_\times < 0$ are ferromagnetic. Based on the numerical results, we also give a numerical estimation of the criticality line. In Fig. 6, the solid curve represents an exponential function fitted to numerical values, which is written as

$$J_\perp = (-0.0768 - 0.0525\cdot J_\times) \times [0.268 - \delta + 0.229\cdot J_\times]^{-1.580+0.830\cdot J_\times}. \quad (9)$$

As a result, the phase transition points decrease rapidly with the increasing δ, especially in areas of large δ, which means that the columnar order is relatively stable in the thermodynamic limit, only a sufficiently large rung coupling can destroy the dimerization on the leg and drives a transition from the CD phase to Haldane phase. Moreover, at a fixed value of δ, the critical values of $J_\perp$ also decrease rapidly with increasing the magnitude of $J_\times$. Hence, the diagonal ferromagnetic frustration strongly favors the CD state over Haldane state. When $J_\times$ equals zero, the fitting function approximately satisfies $J_\perp = -0.0768\cdot(0.268-\delta)^{-1.580}$, with a modest difference from the result $J_\perp = -0.16\cdot(0.259-\delta)^{-1.25}$ in Ref. [19]. These differences may come from differences in numerical methods and boundary conditions.

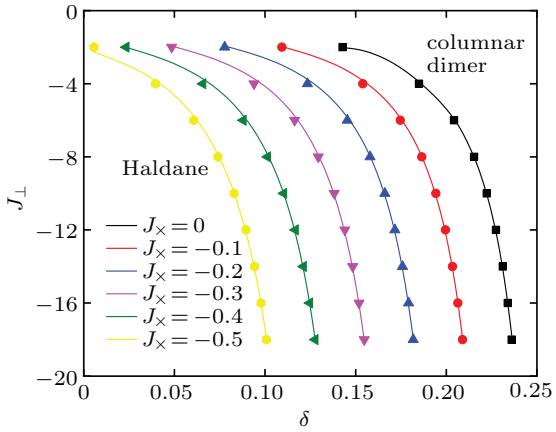


Fig. 6. Ground-state phase diagram of columnar dimerized ladder with ferromagnetic interchain coupling, $J_\perp < 0$, $J_\times < 0$. The simulation results are denoted by symbols and the fitting curves by the solid lines, respectively.

Finally, we discuss the $\delta = 0$ situation, in this case the model of Hamiltonian (1) is reduced to the cross-coupled ladder. What calls for special attention is that a columnar dimerized phase emerges in between the Haldane phase and the rung-singlet when the interchain couplings are ferromagnetic.[14] For the antiferromagnetic ladder, although some results support the existence of the dimerized phase,[13] it is now generally suggested that there is no such a phase.[12]

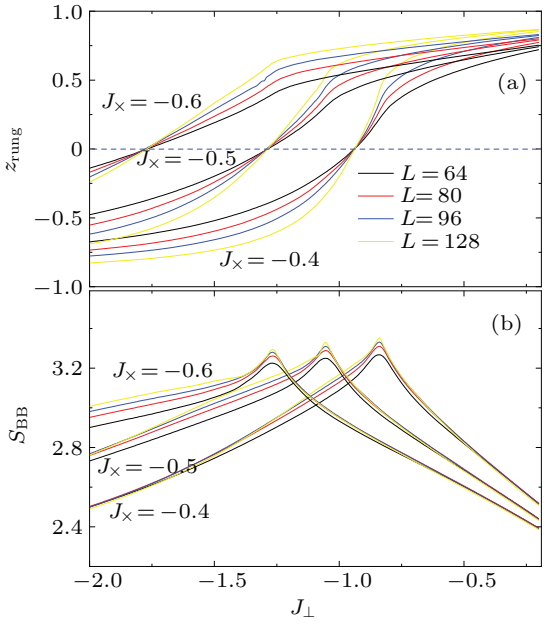


Fig. 7. $J_\perp$ dependence of the (a) $z_{\rm rung}$ and (b) $S_{\rm BB}$ for different system sizes L and diagonal couplings $J_\times$.

In Fig. 7, we present the $J_\perp(<0)$ dependence of the $z_{\rm rung}$ and $S_{\rm BB}$ with different system sizes L and diagonal coupling strengths $J_\times(<0)$. From Fig. 7(a), one can observe the sign of $z_{\rm rung}$ changes from positive to negative values as $J_\perp$ decreases. The crossing point of $z_{\rm rung}$ thereby gives a signature of the critical point between the CD and Haldane phases. It is important to note that the $z_{\rm rung}$ curves present obvious inflection points and especially evident at large system sizes, which are smaller than the values obtained from $z_{\rm rung} = 0$. Compared with Fig. 7(b), one can find that these inflection points correspond strictly to the maximum of $S_{\rm BB}$, which are just the transition points separating RS and CD phases.

Combining the above results, a CD phase intervenes between the RS and Haldane phases. For all values of $J_\times$, the transition from RS phase to Haldane phase with decreasing $J_\perp$ takes place in two steps. Firstly, $S_{\rm BB}$ reaches its maximum while $z_{\rm rung}$ ($z_{\rm diag}$) does not change sign, which denotes that the parity does not change during QPT, so the critical point measured by $S_{\rm BB}$ indicates the RS-CD transition which is caused by level crossing of the low-lying excited states.[35] Then, $z_{\rm rung}$ ($z_{\rm diag}$) changes sign and the CD-Haldane transition occurs, which is induced by the change of parity.

Based on our TOP and $S_{\rm BB}$ results, the ground-state phase diagram of the cross-coupled spin ladder in the thermodynamic limit is demonstrated in Fig. 8. The two phase boundaries distinguish three different quantum phases. The weak and strong $J_\perp$ regions correspond to RS and Haldane phases, respectively, and the CD phase exists in the intermediate region. Our results suggest that the RS-CD phase transition takes place for $J_\perp \lesssim 2J_\times$. Our results are quantitative consistent with the previous conclusions derived in Ref. [14] but with improved precision.

On the other hand, for the antiferromagnetic cross-coupled ladder($J_\perp > 0, J_\times > 0$), the difference of critical points obtained by this two methods is very small (< 0.01, data not shown). Hence, there is no clear evidence of an intermediate phase. The corresponding phase diagram is also presented in Fig. 8.

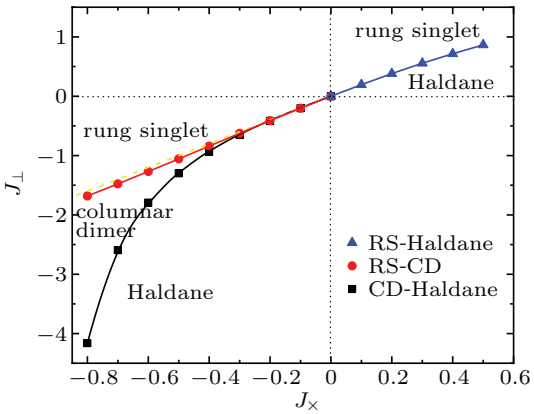


Fig. 8. Ground-state phase diagram of cross-coupled spin ladder. The triangle, circle and rectangular symbols represent RS-Haldane, RS-CD and CD-Haldane transition points, respectively. The solid lines are of guides to the eyes, and the dashed line indicates $J_\perp = 2J_\times$.

5. Conclusion

In summary, we have investigated the QPTs in bond-alternating spin ladder with diagonal frustration $J_\times$ using the DMRG algorithm. We calculate several types of measurements including string order parameter, twist order parameter

and block-block entanglement entropy to verify the different phases and determine the phase boundaries precisely. Our results show that the diagonal frustration $J_\times$ favors dimer phases in bond-alternating spin ladder. We also discuss the situation of ferro-antiferromagnetic cross-coupled spin ladder. We find that the TOPs and quantum entanglement entropy infer two different QPTs, a CD phase appears in between RS and Haldane phase. For the antiferromagnetic ladder, there is no clear evidence of an intermediate phase.

References

[1] Azuma M, Hiroi Z, Takano M, Ishida K and Kitaoka Y 1994 *Phys. Rev. Lett.* **73** 3463
[2] Hong T, Schmidt K P, Coester K, Awwadi F F, Turnbull M M, Qiu Y, Rodriguez-Rivera J A, Zhu M, Ke X, Aoyama C P, Takano Y, Cao H B, Tian W, Ma J, Custelcean R, Zhou H D and Matsuda M 2014 *Phys. Rev. B* **89** 174432
[3] Rao G N, Sankar R, Singh A, Muthuselvam I P, Chen W T, Singh V N, Guo G Y and Chou F C 2016 *Phys. Rev. B* **93** 104401
[4] Gibbs A S, Yamamoto A, Yaresko A N, Knight K S, Yasuoka H, Majumder M, Baenitz M, Saines P J, Hester J R, Hashizume D, Kondo A, Kindo K and Takagi H 2017 *Phys. Rev. B* **95** 104428
[5] Glamazda A, Choi Y S, Do S H, Lee S, Lemmens P, Ponomaryov A N, Zvyagin S A, Wosnitza J, Sari D P, Watanabe I and Choi K Y 2017 *Phys. Rev. B* **95** 184430
[6] Macdougal D, Gibbs A S, Ying T, Wessel S, Walker H C, Voneshen D, Mila F, Takagi H and Coldea R 2018 *Phys. Rev. B* **98** 174410
[7] Starykh O A and Balents L 2004 *Phys. Rev. Lett.* **93** 127202
[8] Azzouz M, Shahin K and Chitov G Y 2007 *Phys. Rev. B* **76** 132410
[9] Hung H H, Gong C D, Chen Y C and Yang M F 2006 *Phys. Rev. B* **73** 224433
[10] Kim E H, Legeza Ö and Sólyom J 2008 *Phys. Rev. B* **77** 205121
[11] Barcza G, Legeza Ö, Noack R M and Sólyom J 2012 *Phys. Rev. B* **86** 075133
[12] Luo Q, Zhao J Z and Wang X Q 2019 *Phys. Rev. B* **100** 121111
[13] Liu G H, Wang H L and Tian G S 2008 *Phys. Rev. B* **77** 214418
[14] Hikihara T and Starykh O A 2010 *Phys. Rev. B* **81** 064432
[15] Dagotto E and Rice T M 1996 *Science* **271** 618
[16] White S R, Noack R M and Scalapino D J 1994 *Phys. Rev. Lett.* **73** 886
[17] Martín-Delgado M A, Shankar R and Sierra G 1996 *Phys. Rev. Lett.* **77** 3443
[18] Okamoto K 2003 *Phys. Rev. B* **67** 212408
[19] Almeida J, Martín-Delgado M A and Sierra G 2007 *Phys. Rev. B* **76** 184428
[20] Chitov G Y, Ramakko B W and Azzouz M 2008 *Phys. Rev. B* **77** 224433
[21] Gibson S J, Meyer R and Chitov G Y 2011 *Phys. Rev. B* **83** 104423
[22] White S R 1992 *Phys. Rev. Lett.* **69** 2863
[23] White S R 1993 *Phys. Rev. B* **48** 10345
[24] Nakamura M and Todo S 2002 *Phys. Rev. Lett.* **89** 077204
[25] Almeida J, Martín-Delgado M A and Sierra G 2008 *J. Phys. A: Math. Theor.* **41** 485301
[26] Feiguin A E, Riera J A, Dobry A and Ceccatto H A 1997 *Phys. Rev. B* **56** 14607
[27] den Nijs M and Rommelse K 1989 *Phys. Rev. B* **40** 4709
[28] Shelton D G, Nersesyan A A and Tsvelik A M 1996 *Phys. Rev. B* **53** 8521
[29] Wootters W K 1998 *Phys. Rev. Lett.* **80** 2245
[30] Gu S J, Deng S S, Li Y Q and Lin H Q 2004 *Phys. Rev. Lett.* **93** 086402
[31] Wu L A, Sarandy M S and Lidar D A 2004 *Phys. Rev. Lett.* **93** 250404
[32] Sólyom J and Legeza Ö 2006 *Phys. Rev. Lett.* **96** 116401
[33] Legeza Ö, Sólyom J, Tincani L and Noack R M 2007 *Phys. Rev. Lett.* **99** 087203
[34] Molina R A and Schmitteckert P 2007 *Phys. Rev. B* **75** 235104
[35] Tian G S and Lin H Q 2003 *Phys. Rev. B* **67** 245105